Mixed Mosaic Membranes Prepared by Layer-by-Layer Assembly for Ionic Separations

Sahadevan Rajesh,[†] Yu Yan,[†] Hsueh-Chia Chang,[†] Haifeng Gao,[‡] and William A. Phillip*[,†]

[†]Department of Chemical and Biomolecular Engineering and [‡]Department of Chemistry and Biochemistry, University of Notre Dame, Notre Dame, Indiana 46556-5637, United States

ABSTRACT Charge mosaic membranes, which possess distinct cationic and anionic domains that traverse the membrane thickness, are capable of selectively separating dissolved salts from similarly sized neutral solutes. Here, the generation of charge mosaic membranes using facile layer-by-layer assembly methodologies is reported. Polymeric nanotubes with pore walls lined by positively charged polyethylenimine moieties or negatively charged poly(styrenesulfonate) moieties were prepared *via* layer-by-layer assembly using track-etched membranes as sacrificial templates. Subsequently, both types of nanotubes were deposited on a porous support in order to produce mixed mosaic membranes. Scanning electron microscopy demonstrates that the facile deposition techniques implemented result in nanotubes that are vertically aligned without overlap between adjacent elements. Furthermore, the nanotubes span the thickness of the mixed mosaic membranes. The effects of this unique nanostructure are reflected in the transport characteristics of the mixed mosaic membranes. The hydraulic permeability of the mixed mosaic membranes in piezodialysis operations was 8 L m^{-2} h^{-1} bar^{-1}. Importantly, solute rejection experiments demonstrate that the mixed mosaic membranes are more permeable to ionic solutes than similarly sized neutral molecules. In particular, negative rejection of sodium chloride is observed (*i.e.*, the concentration of NaCl in the solution that permeates through a mixed mosaic membrane is higher than in the initial feed solution). These properties illustrate the ability of mixed mosaic membranes to permeate dissolved ions selectively without violating electroneutrality and suggest their utility in ionic separations.

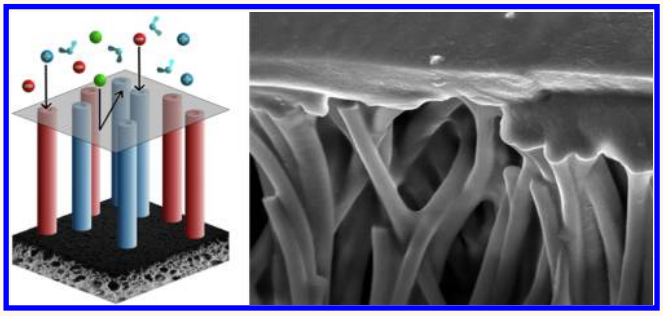

KEYWORDS: charge mosaic membranes · layer-by-layer assembly · nanotubes · ion permeation · composite membranes

The separation of dissolved ions from aqueous solutions is critical to many technologies that are necessary to meet the growing demand for water and energy sustainably. For example, seawater desalination,[1] wastewater reclamation,[2] recycling metals from expired batteries,[3] and the processing of biofuels involve steps that rely on separating ionic species from a mixture selectively. The importance of this class of separations is well-recognized, and membranes capable of separating ions and water based on the size difference between the molecules have been developed.[4,5] Reverse osmosis desalination, which is currently the most energy efficient large-scale desalination process, is one example of a process that relies on this type of membrane that allows water to permeate, but hinders the passage of ions.[1] Given the importance of this application, researchers are continually developing novel materials such as lyotropic liquid crystals,[6,7] self-assembled block polymers,[8,9] carbon nanotubes,[10,11] graphene,[12,13] and aquaporins[14] in attempts to provide greater control over the size and distribution of free volume elements in these size-selective membranes. In systems where the dissolved ions are the valued product to be recovered or the ions are present at dilute concentrations, there are significant operational advantages to implementing a membrane that permeates ions more rapidly than water and/or neutral solutes.[15−18] In these cases, however, the development of advanced materials focused on improving size-selectivity will not lead to membranes with the desired properties. Instead, it is necessary to control the nanostructure and

* Address correspondence to wphillip@nd.edu.

Received for review August 22, 2014 and accepted December 3, 2014.

Published online December 03, 2014
10.1021/nn504736w

the chemical functionality to produce membranes that permeate ions preferentially.

Charge mosaic membranes are an alternative class of membranes that are more permeable to electrolytes than neutral molecules of comparable molecular weight.[15−22] These membranes consist of bicontinuous positively charged and negatively charged domains. According to the phenomenological theory proposed by Sollner,[23] this unique microstructure allows anions and cations to permeate through their counter-charged regions without violating the macroscopic constraint of electroneutrality, and as a result, a circulation current develops between the individual ionic elements that speeds the permeation of electrolytes. In the last four decades, attempts have been made to develop charge mosaics from a variety of materials including self-assembled graft and block polymers,[15,21,22] ion exchange resins embedded in permeable matrices,[17,18] and electrospun polymers.[19] However, the fabrication of highly effective charge mosaics from these systems has proven difficult due to the need to orient the ionic domains perpendicular to the surface and the morphological changes induced during the harsh chemical treatments required to introduce charged moieties into some of the membranes. Therefore, it is necessary to develop a method to prepare charge mosaics with well-defined nanostructures and chemical functionality to advance this novel class of membranes relative to the current state of the art.

Layer-by-layer (LbL) assembly is a simple technique that uses the repeated, sequential deposition of unlike materials to build up multilayer constructs.[24] This technique, which often exploits the electrostatic interaction between oppositely charged species, is a powerful and versatile method for the formation of nanostructured materials (*e.g.*, nanorods and nanotubes) and polymeric thin films with tailored functionality and controlled dimensions.[25−27] These materials have been implemented in a wide range of applications including antibacterial coatings,[28−30] drug delivery,[31] protective barriers,[32,33] and gas separation[34] and nanofiltration membranes.[35−37] Several prior studies regarding LbL-derived membranes have demonstrated that it is possible to tune the permselectivity of the membranes by the judicious selection of the deposited materials and conditions implemented during LbL assembly.[34−36,38−40] However, the technique has not been exploited to control both the nanostructure and chemical functionality of next-generation membranes simultaneously. In particular, mosaic membranes, which contain multiple domains of unique chemical design that span the membrane thickness, have not been demonstrated using the LbL methodology, despite the promise of this class of membranes.

In this study, LbL assembly is used to prepare charge mosaic membranes. The LbL methodology is used to construct charged nanotubes. Subsequently, these nanotubes are oriented and attached to a porous support membrane to produce mixed mosaic membranes (MMMs). The ultimate nanostructure of the MMMs is shown schematically in Figure 1. Because the MMMs have both positively charged and negatively charged domains that span the membrane thickness, ionic species permeate more rapidly than similarly sized neutral molecules, which make the MMMs an excellent candidate for the separation of ionic solutes from aqueous solutions.

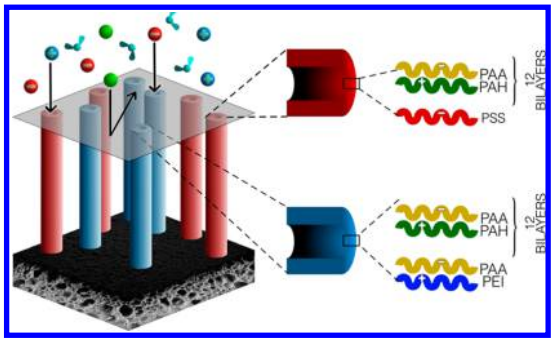

Figure 1. Schematic of the mixed mosaic membranes (MMMs) prepared using LbL assembly. Cationic (blue) and anionic (red) nanotubes are aligned vertically on a support membrane, and a sealing layer is applied to prevent convective flow through the interstitial regions between the nanotubes. Dissolved ions (blue and red spheres) can permeate through nanotubes lined by moieties with the opposite charge, which results in higher ionic permeabilities compared to the permeability of neutral molecules (green spheres). Anionic and cationic polymeric nanotubes were prepared by terminating the multilayer assembly with negatively charged poly(styrenesulfonate) and positively charged polyethylenimine, respectively.

RESULTS AND DISCUSSION

The fabrication of MMMs began by using polycarbonate track etched (PCTE) membranes as a template for the preparation of "cationic" and "anionic" nanotubes. The PCTE membranes were coated with an initial layer of polyethylenimine (PEI). Then, 12 bilayers of poly(acrylic acid) (PAA) and poly(allylamine hydrochloride) (PAH) were deposited within the pores of the PCTE membrane by dip coating.[41,42] Lastly, the membrane was placed in a solution of PEI or poly(styrenesulfonate) (PSS) to terminate the multilayer buildup and form nanotubes with cores lined by positively charged or negatively charged functional groups, respectively (Figure S1). The PEI-terminated nanotubes, which have a final composition of [PEI $(PAA/PAH)_{12.5}$ PEI], are referred to as "cationic", and the PSS-terminated nanotubes, which have a final composition of [PEI $(PAA/PAH)_{12.0}$ PSS], as "anionic". Prior to the dissolution of the PCTE template, the nanotubes were cross-linked by heat treatment.[41,43] As shown in Figure 2, the outer diameter and length of the resulting nanotubes are around 400 nm and 10 μm, respectively, which is in good agreement with the pore diameter and thickness

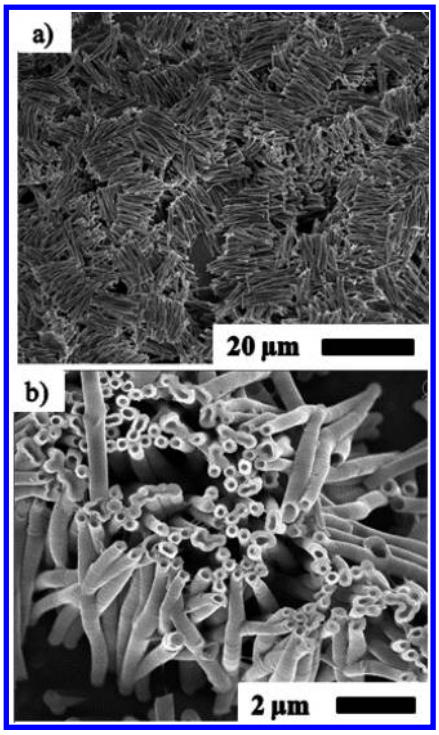

Figure 2. Scanning electron micrographs of the polymeric nanotubes obtained using the LbL process. PAA and PAH, which can be cross-linked upon heating, were used to generate the robust wall of the polymeric nanotubes. A track-etched membrane with a thickness of 10 μm and a pore diameter of 400 nm was used as a template for the preparation of the nanotubes.

of the PCTE template. The thickness of the walls of the nanotubes depends strongly on the deposition conditions (*e.g.*, assembly pH and ionic strength, number of bilayers, and the presence of divalent ions), as shown in Figures S2 and S3 of the Supporting Information. The nanotubes used to prepare MMMs were deposited from solutions containing 40 mM polyelectrolyte, 35 mM $CaCl_2$, and 0.5 M NaCl. The pH of the solution was adjusted to 5.5 using NaOH and HCl as needed.

Because the surface charge on the inside of the nanotubes is critical to the function of charge mosaic membranes, its sign was determined using streaming current measurements. A detailed description of the experimental setup used for the measurements is available in the prior literature.[44] Briefly, a PCTE template was placed between two compartments filled with a 1 mM KCl solution. Pressure was applied on the compartment connected to the positive terminal of the current meter, and the resulting current was measured. Figure 3 displays the results of these measurements made as a function of solution pH for templates containing PSS-terminated and PEI-terminated nanotubes. Streaming current measures the difference between the flux of cations and the flux of anions through a charged pore under hydrodynamic flow. When pressure is applied on the side of the experimental setup that is connected to the positive terminal of the current

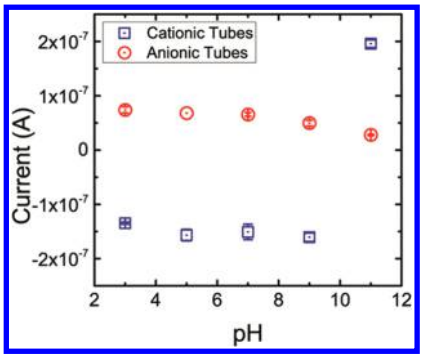

Figure 3. Streaming current measured as a function of pH for the PSS-terminated and PEI-terminated nanotubes. The streaming current was measured using a 1 mM KCl solution. A pressure of 0.28 bar was applied on the side of the experimental system connected to the positive terminal of the current meter. The pH of the KCl solution was adjusted by adding HCl or KOH. Error bars represent the standard deviation between multiple measurements.

meter, a positive current indicates that a membrane is negatively charged (*i.e.*, it is preferentially permeable to cations). From Figure 3, flow through the PSS-terminated nanotubes resulted in a nearly constant positive current over the pH range studied, which is consistent with pores lined by sulfonic acid moieties.[45]

The streaming current for the PEI-terminated nanotubes is negative for solutions from pH 3 to pH 9, and at pH 11, it becomes positive. The negative streaming current at lower pH values can be attributed to the protonation of the amine groups of PEI, which is consistent with a number of studies in the literature that report a positive charge for PEI at low pH.[46,47] These studied also observe that above pH 10.5 most of the amine groups are deprotonated, resulting in PEI macromolecules that possess negligible charge. Thus, it is reasonable to speculate that anion adsorption onto neutral PEI results in the positive streaming current at pH 11. Subsequent transport measurements were made using DI water, which has a pH of ~5.5. At this pH, the cationic and anionic nanotubes possess a positive and negative surface charge, respectively.

A highly porous polyacrylonitrile (PAN) ultrafiltration membrane was used as a support for the MMMs. Prior to fabrication the PAN support was soaked in a 1 M NaOH solution for 1 h. After rinsing the support with water, a PCTE membrane containing cationic nanotubes was placed on top of the PAN support. The layered system was then heated to 80 °C under air for 1 h to facilitate the attachment of the cationic nanotubes to the surface of the PAN support. After cooling to room temperature, the PCTE membrane that was used as a structural template for the cationic nanotubes was removed selectively by immersing the system in dichloromethane. This process produced a PAN support with cationic nanotubes fixed to the surface. Subsequently, anionic nanotubes were attached to the PAN support using the same process

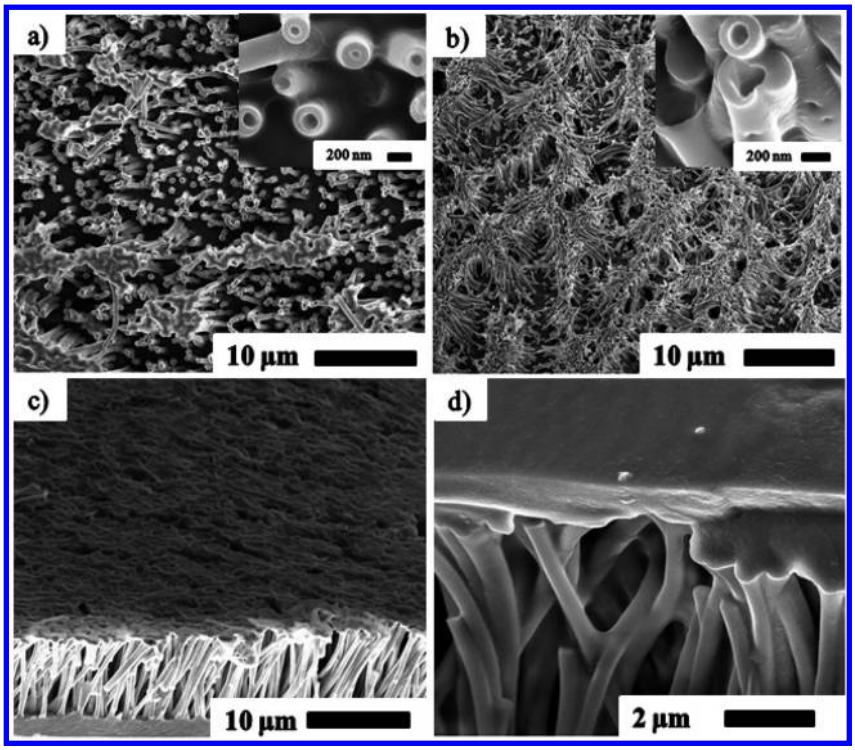

Figure 4. Scanning electron micrographs of MMMs. (a) PEI-terminated nanotubes deposited on the PAN support; (b) PEI-terminated and PSS-terminated nanotubes deposited on the PAN support; (c, d) the MMM after the formation of the sealing layer on top of the PEI-terminated and PSS-terminated nanotubes. MMMs were produced by functionalizing the PAN support with PEI-terminated and PSS-terminated nanotubes sequentially before applying the sealing layer. The sealing layer comprised 3.5 bilayers of PAH/PAA deposited *via* LbL self-assembly. The insets of (a) and (b) show the deposited nanotubes at higher magnification.

with a PCTE membrane containing anionic nanotubes. A detailed description of the method is included in the Supporting Information (Figures S4 and S5). Finally, in order to block the convective flow through the interstitial space between the nanotubes, a sealing layer comprising 3.5 bilayers of PAH/PAA deposited on top of the nanotubes was formed.[48]

SEM micrographs of the membrane after each step are displayed in Figure 4. Figure 4a shows a micrograph of the cationic tubes attached to the PAN support. The inner diameter of the nanotubes was in the range 15−20 nm, and all the nanotubes were aligned with their long axes normal to the support membrane surface. Figure 4b shows a micrograph of the MMM after the sequential deposition of cationic and anionic nanotubes. As can be seen in Figure 4b, using the simple methodology described here, it is possible to arrange these elements of unique chemical design without overlap. Figure 4c and d are micrographs of the MMM after the formation of the sealing layer. These micrographs demonstrate that the LbL method used to produce the MMMs was extremely effective in the vertical alignment of polymeric nanotubes with distinct chemical functionality over the entire surface of the MMMs.

The transport properties (*i.e.*, hydraulic permeability and solute rejection) of the MMMs were measured using an Amicon stirred cell, which has an exposed membrane area of 4.9 cm^2. In addition to the MMMs, cationic composite, anionic composite, and control membranes were prepared and tested. The cationic membranes comprise a sealing layer applied on top of PEI-terminated nanotubes, the anionic membranes comprise a sealing layer applied on top of PSS-terminated nanotubes, and the control membranes were prepared by depositing a sealing layer directly onto the PAN support.

Hydraulic permeability was determined from the slope of pure water flux *versus* applied pressure. Pure water flux was calculated using eq 1:

$$J_w = \frac{V_{permeate}}{A_m t} \quad (1)$$

where J_w is the pure water flux, $V_{permeate}$ is the volume of permeate solution collected, A_m is the membrane area, and t is the time. All the membranes tested possess hydraulic permeabilities around 5 L m^{-2} h^{-1} bar^{-1} (Figure S6). The permeabilities of the composite membranes (8 L m^{-2} h^{-1} bar^{-1}) were slightly higher than the permeability of the control membrane (4 L m^{-2} h^{-1} bar^{-1}), which may be a result of the nanotubes acting as a "gutter layer" between the sealing and support layers.[48]

The influence of steric and electrostatic interactions on the solute rejection characteristics of the membranes was probed by challenging the MMMs with

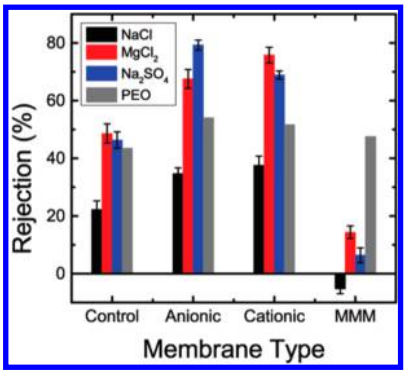

Figure 5. Comparison of solute rejection for charged and neutral solutes between four different membranes. The control membrane was made by depositing the sealing layer (*i.e.*, 3.5 bilayers of PAH and PAA) directly onto the support membrane, anionic membranes were produced by functionalizing the support with PSS-terminated nanotubes then applying the sealing layer, cationic membranes were produced by functionalizing the support with PEI-terminated nanotubes then depositing the sealing layer, and the MMMs were produced by functionalizing the PAN support with both PEI-terminated and PSS-terminated nanotubes before applying the sealing layer. Poly(ethylene oxide) (PEO) with a molar mass of 2.0 kg mol^{-1} was used as the neutral solute. Three different charged solutes were used: $MgCl_2$, Na_2SO_4, and NaCl. The salt was dissolved in the feed solution at a concentration of 10 mM. All experiments were carried out at an applied pressure of 4 bar. Error bar represents the standard deviation (n = 2).

solutions containing a dissolved salt [*i.e.*, sodium chloride (NaCl), magnesium chloride ($MgCl_2$), or sodium sulfate (Na_2SO_4)] and/or neutral poly(ethylene oxide) (PEO). Salt concentrations of 0.1 and 10 mM and a PEO concentration of 1 g L^{-1} were used. During each experiment, samples of the feed and permeate solutions were collected; ion concentrations were measured using a conductivity probe and ion chromatography; and the concentration of PEO was measured using a total organic carbon analyzer. The percent rejection, R, for each solute was calculated using eq 2:

$$R(\%) = \left(1 - \frac{c_{permeate}}{c_{feed}}\right) \times 100 \qquad (2)$$

where c_{feed} is the concentration of solute in the feed and $c_{permeate}$ is the concentration of solute in the permeate.

The results of solute rejection tests conducted with 10 mM salt solutions and a 1 g L^{-1} PEO solution are presented in Figure 5. All of the membranes rejected ~50% of the dissolved PEO, which was selected because it is a neutral molecule that interacts minimally with its environment. Therefore, it is rejected primarily due to size exclusion. The comparable rejection of PEO across all of the membranes suggests that they have similarly sized free volume elements that reject solutes by steric exclusion. Noticeably, the rejection of charged solutes was significantly different across all of the membranes.

The control, cationic composite, and anionic composite membranes all functioned as nanofiltration membranes rejecting monovalent and divalent salts partially. The control membrane performed comparably to other NF membranes in the literature that were made using LbL assembly.[35,36,49] Interestingly, the presence of charged nanotubes under the PAH/PAA sealing layer affected the solute rejection greatly. For example, the anionic composite membrane and cationic composite membrane rejected dissolved salts more effectively than the control membrane alone, which is likely a result of the electrostatic interactions between the nanotubes and solutes (*i.e.*, Donnan exclusion). The fact that the anionic and cationic membranes demonstrate maximum rejections of 79.4% for Na_2SO_4 and 75.8% for $MgCl_2$, respectively, supports this hypothesis.

In contrast to the other membranes, the MMMs did not reject dissolved ions effectively. The divalent salts were rejected to a lower extent than the PEO molecule ($R(Na_2SO_4)$ = 6.4%, $R(MgCl_2)$ = 14.2%, and R(PEO) = 47.6%) even though their hydrodynamic radii are comparable[7,50] (~0.9 nm). This difference in permeability between the neutral and charged solutes illustrates the role that electrostatic interactions have in determining the separation efficiency of the MMMs. The negative rejection of NaCl (R(NaCl) = −5.3%), which indicates that the NaCl ions permeated through the membrane more rapidly than water, reinforces the importance of the electrostatic interactions. It also indicates that the MMM is capable of enriching the ion concentration in the permeating solution.

The solute rejection results described above were observed for experiments conducted with single solute solutions as well as mixed solute (*i.e.*, containing both a dissolved salt and PEO) solutions (Figure S7). Additionally, the difference in percent rejection between feed solutions at 0.1 and 10 mM was insignificant (Figure S8). We hypothesize that this is due to the ion-selective nature of the nanotubes. In order to balance the surface charge on the walls of the nanotubes, a sufficient concentration of ions must be present within the core volume of the nanotubes. It has been demonstrated previously that this constraint results in a constant conductivity across a nanopore for solutions below a critical concentration. For a 200 nm nanochannel, this concentration is around 10 mM, and the critical concentration increases with decreases in pore size.[51] Therefore, it is likely that the critical concentration for the ~20 nm nanotubes described here is greater than 10 mM. Future studies will consider the effects of this phenomenon in greater detail.

The discussion above implies that the charge on the interior surface of the nanotubes determines the performance of the composite and mosaic membranes. However, the fabrication of all the nanotubes began

with the deposition of a PEI layer. Therefore, it is reasonable to hypothesize that the positive charge on the exterior of the nanotubes will affect membrane performance. If this charge played a significant role in the performance of the mosaic membranes, we anticipate that the anionic composite membranes would behave like a charge mosaic because of the positively charged exterior surface and negatively charged interior surface. However, the anionic composite membrane performs in a manner similar to a negatively charged nanofiltration membrane. This is not conclusive evidence that the charge on the exterior of the nanotubes plays no role in the performance of the mosaic membranes, but it does suggest that the charge on the interior of the nanotubes is the dominant factor determining the performance of composite and mosaic membranes. Further experiments should elucidate clearly the effects of the charge on the exterior of the nanotubes on membrane performance.

CONCLUSIONS

The present investigation reports the successful fabrication of charge mosaic membranes using simple LbL assembly techniques. These techniques are used to produce mosaic membranes that contain uniformly oriented nanotubes, which are lined by moieties of unique chemical design. In this study, this ability is used to fabricate a membrane that contains both nanometer-sized cationic and anion domains. This novel nanostructure results in mosaic membranes that (1) demonstrate higher ionic fluxes compared to similarly sized neutral molecules and (2) are capable of enriching the ion concentration in the solution that permeates through the membrane. As such, this membrane platform and the unique transport characteristics it exhibits, provide an opportunity to study a novel ion permeation paradigm, which we anticipate provides significant opportunities for a broad range of separations and sensing applications.

METHODS

Materials. Polycarbonate track-etched membranes with a pore diameter of 400 nm were purchased from Millipore. Poly(sodium 4-styrenesulfonate) (MW = 70 kg mol^{-1}) and poly(acrylic acid) (MW = 1.8 kg mol^{-1}) (Sigma-Aldrich), poly(allylamine hydrochloride) (MW = 120 kg mol^{-1}) (Alfa-Aesar), and polyethylenimine (MW = 25 kg mol^{-1}; 25% aqueous solution) (Acros Organics) were all used as received. Polyacrylonitrile ultrafiltration (PAN UF) membranes (PAN 400) were purchased from ULTURA. Poly(ethylene oxide) (MW = 2.1 kg mol^{-1}) was purchased from Polymer Source, Inc. (Montreal, Canada). Sodium chloride (NaCl), potassium chloride (KCl), copper chloride ($CuCl_2$), calcium chloride ($CaCl_2$), magnesium chloride ($MgCl_2$), and sodium sulfate (Na_2SO_4) were purchased from Sigma-Aldrich. Deionized water (DI water, 18.2 MΩ) (Milli-Q Advantage A10, Millipore Corporation) was used to prepare all aqueous solutions. Dichloromethane was purchased from Sigma-Aldrich.

Nanotube Preparation. Solutions containing 40 mM polyelectrolyte (based on the repeat unit molecular weight), 35 mM $CaCl_2$ (or $CuCl_2$), and 0.5 M NaCl in DI water were used to fabricate nanotubes.[39,41,43,52] After dissolving the polyelectrolyte, the pH of the solution was adjusted to 5.5 using NaOH or HCl. Nanotube fabrication began by immersing the PCTE substrate in a solution of PEI for 60 min followed by washing with DI water for 2 min. The substrate was then dipped into a solution of PAA for 60 min followed by rinsing with DI water for 2 min. Subsequently, the PCTE was immersed in a solution of PAH for 60 min and then washed with DI water for 2 min. Sonication was applied at the start of each polyelectrolyte adsorption step. One PAA/PAH deposition cycle was defined as a bilayer, and the process was repeated until the desired number of bilayers was formed. The bilayer assembly was terminated with PSS and PEI to fabricate anionic and cationic tubes, respectively. After drying the PCTE substrate, the polyelectrolyte deposited on the top and bottom surface was removed by plasma etching. The bilayers that made up the nanotube walls were then cross-linked at 160 °C under air for 24 h. Polymer nanotubes were released by the dissolution of template PCTE membranes in dichloromethane.

Mosaic Membrane Preparation. Charge mosaic membranes were fabricated using PAN UF membranes as a support. The PAN substrate was soaked in 1 M NaOH at 55 °C for 1 h and rinsed with DI water. A PCTE membrane containing PEI-terminated nanotubes was then placed on the NaOH-treated PAN support. It is important to ensure that the PCTE membrane lies smoothly on top of the PAN support (*i.e.*, it should be wrinkle-free). The PAN–PCTE composite was put into an oven at 80 °C for 60 min before being immersed in dichloromethane to dissolve the PCTE membrane away selectively. Subsequently, PSS-terminated tubes were deposited onto the PAN support using the same process. The sealing layer of the membrane was formed using layer-by-layer assembly to deposit 3.5 bilayers of PAH and PAA on top of the vertically aligned nanotubes. Cationic composite membranes, anionic composite membranes, and control membranes were also prepared using these techniques.

Characterization. Micrographs were obtained using a high-resolution Magellan 400 field emission scanning electron microscope. Prior to imaging, samples were dried and then sputter coated with a thin (~1.5 nm) layer of iridium. The streaming current of the nanotubes (I_{str}) was measured using an experimental setup that is detailed in the prior literature.[44] A PCTE template containing nanotubes was clamped between two compartments that were filled with a 1 mM KCl solution. One of the compartments was airtight, and a pressure of 0.28 bar was applied to drive the flow of solution through the nanotubes. Ag/AgCl electrodes were used to connect the two cells, and I_{str} was recorded directly by a Keithley model 2636 dual-channel system. The pH of the KCl solution was modified from pH 3 to pH 11 using HCl or KOH.

Transport Studies. Water flux and solute rejection tests were performed using an Amicon stirred cell (model 8010) with an exposed membrane area of 4.9 cm^2. An applied pressure from 1 to 4 bar was generated using nitrogen gas. The flux of pure water was calculated by measuring the mass of permeating DI water at regular time intervals. Solute rejection was evaluated by challenging the membranes with solutions containing dissolved salts ($MgCl_2$, Na_2SO_4, or NaCl) and/or neutral PEO. Salt concentrations of 0.1 and 10 mM and a PEO concentration of 1 g L^{-1} were used. The first 1.5 mL of permeate was discarded to avoid contamination between experimental runs. Samples of the feed and permeate solutions were collected, and the ion concentrations were measured using a conductivity probe and ion chromatography (IA64 Thermo Dionex ICS-5000); the concentration of PEO was measured using a total organic carbon analyzer (Shimadzu TOC-V_{CSH}).

Conflict of Interest: The authors declare no competing financial interest.

Supporting Information Available: Detailed descriptions of the polyelectrolytes and the effects of deposition solutions on the structure of polymeric nanotubes. Schematic and description of

the fabrication methodology used to produce composite and mixed mosaic membranes. A plot of water flux *vs* applied pressure for all of the membranes tested. Solute rejection data for membranes challenged with mixed solute solutions and membranes challenged with 0.1 mM salt solutions. This material is available free of charge *via* the Internet at http://pubs.acs.org.

Acknowledgment. We acknowledge the support of the Center for Sustainable Energy at Notre Dame. We thank the Notre Dame Integrated Imaging Facility (NDIIF) and the Center for Environmental Science and Technology (CEST) at Notre Dame; portions of this research were performed with equipment from these facilities. Special thanks to Sherwood Benavides for producing the schematic of the MMMs.

REFERENCES AND NOTES

1. Elimelech, M.; Phillip, W. A. The Future of Seawater Desalination: Energy, Technology, and the Environment. *Science* **2011**, *333*, 712–717.
2. Shannon, M.; Bohn, P.; Elimelech, M.; Georgiadis, J.; Marinas, B.; Mayes, A. Science and Technology for Water Purification in the Coming Decades. *Nature* **2008**, *452*, 301–310.
3. Iizuka, A.; Yamashita, Y.; Nagasawa, H.; Yamasaki, A.; Yanagisawa, Y. Separation of Lithium and Cobalt From Waste Lithium-Ion Batteries *via* Bipolar Membrane Electrodialysis Coupled with Chelation. *Sep. Purif. Technol.* **2013**, *113*, 33–41.
4. Geise, G. M.; Lee, H. S.; Miller, D. J.; Freeman, B. D.; Mcgrath, J. E.; Paul, D. R. Water Purification by Membranes: The Role of Polymer Science. *J. Polym. Sci., Polym. Phys.* **2010**, *48*, 1685–1718.
5. Geise, G. M.; Park, H. B.; Sagle, A. C.; Freeman, B. D.; McGrath, J. E. Water Permeability and Water/Salt Selectivity Tradeoff in Polymers for Desalination. *J. Membr. Sci.* **2011**, *369*, 130–138.
6. Hatakeyama, E. S.; Gabriel, C. J.; Wiesenauer, B. R.; Lohr, J. L.; Zhou, M. J.; Noble, R. D.; Gin, D. L. Water Filtration Performance of a Lyotropic Liquid Crystal Polymer Membrane with Uniform, Sub-1-nm Pores. *J. Membr. Sci.* **2011**, *366*, 62–72.
7. Zhou, M. J.; Nemade, P. R.; Lu, X. Y.; Zeng, X. H.; Hatakeyama, E. S.; NobleR. D.; Gin, D. L. New Type of Membrane qMaterial for Water Desalination Based on a Cross-Linked Bicontinuous Cubic Lyotropic Liquid Crystal Assembly. *J. Am. Chem. Soc.* **2007**, *129*, 9574–9575.
8. Gopinadhan, M.; Deshmukh, P.; Choo, Y.; Majewski, P. W.; Bakajin, O.; Elimelech, M.; Kasi, R. M.; Osuji, C. O. Thermally Switchable Aligned Nanopores by Magnetic-Field Directed Self-Assembly of Block Copolymers. *Adv. Mater.* **2014**, 10.1002/adma.201401569.
9. Mulvenna, R. A.; Weidman, J. L.; Jing, B.; Pople, J. A.; Zhu, Y.; Boudouris, B. W.; Phillip, W. A. Tunable Nanoporous Membranes with Chemically-Tailored Pore Walls from Triblock Polymer Templates. *J. Membr. Sci.* **2014**, 10.1016/j.memsci.2014.07.021.
10. Hinds, B.; Chopra, N.; Rantell, T.; Andrews, R.; Gavalas, V.; Bachas, L. Aligned Multiwalled Carbon Nanotube Membranes. *Science* **2004**, *303*, 62–65.
11. Majumder, M.; Chopra, N.; Hinds, B. Effect of Tip Functionalization on Transport through Vertically Oriented Carbon Nanotube Membranes. *J. Am. Chem. Soc.* **2005**, *127*, 9062–9070.
12. Joshi, R.; Carbone, P.; Wang, F.; Kravets, V.; Su, Y.; Grigorieva, I.; Wu, H.; Geim, A.; Nair, R. Precise and Ultrafast Molecular Sieving through Graphene Oxide Membranes. *Science* **2014**, *343*, 752–754.
13. Mi, B. Graphene Oxide Membranes for Ionic and Molecular Sieving. *Science* **2014**, *343*, 740–742.
14. Kumar, M.; Grzelakowski, M.; Zilles, J.; Clark, M.; Meier, W. Highly Permeable Polymeric Membranes Based on the Incorporation of the Functional Water Channel Protein Aquaporin Z. *Proc. Natl. Acad. Sci. U.S.A.* **2007**, *104*, 20719–20724.
15. Fujimoto, T.; Ohkoshi, K.; Miyaki, Y.; Nagasawa, M. A New Charge-Mosaic Membrane From a Multiblock Copolymer. *Science* **1984**, *224*, 74–76.
16. Ishizu, K.; Amemiya, M. Transport of Elelctrolytes through Charge Mosaic Composite Membranes. *J. Membr. Sci.* **1992**, *65*, 129–140.
17. Weinstein, J. N.; Caplan, S. R. Charge-Mosaic Membranes: Enhanced Permeability and Negative Osmosis with a Symmetrical Salt. *Science* **1968**, *161*, 70–72.
18. Weinstein, J. N.; Caplan, S. R. Charge-Mosaic Membranes: Dialytic Separation of Electrolytes from Nonelectrolytes and Amino Acids. *Science* **1970**, *169*, 296–298.
19. Chen, Y.; Cui, Y.; Jia, Y.; Zhan, K.; Zhang, H.; Chen, G.; Yang, Y.; Wu, M.; Ni, H. Preparation of Charged Mosaic Membrane of Sodium Polystyrene Sulfonate and Poly(4-vinyl pyridine) by Conjugate Electrospinning. *J. Appl. Polym. Sci.* **2014**, *131*, 40716.
20. Higa, M.; Masuda, D.; Kobayashi, E.; Nishimura, M.; Sugio, Y.; Kusudou, T.; Fujiwara, N. Charge Mosaic Membranes Prepared from Laminated Structures of PVA-Based Charged Layers - 1. Preparation and Transport Properties of Charged Mosaic Membranes. *J. Membr. Sci.* **2008**, *310*, 466–473.
21. Kawaktoh, H.; Kakimoto, M.; Tanioka, A.; Inoue, T. Charge-Mosaic Memebrane from a Polymer Blend with a Modulated Structure. *Macromolecules* **1988**, *21*, 625–628.
22. Miyaki, Y.; Nagamatsu, H.; Iwata, M.; Ohkoshi, K.; Se, K.; Fujimoto, T. Artificial Memembranes from Multiblock Copolymers 3 Preparation and Characterization of Charge-Mosaic Membranes. *Macromolecules* **1984**, *17*, 2231–2236.
23. Sollner, K. Mosaic Membranes. *Biochem. Z.* **1932**, *244*, 370–381.
24. Decher, G. Fuzzy Nanoassemblies: Toward Layered Polymeric Multicomposites. *Science* **1997**, *277*, 1232–1237.
25. Zhang, L.; Vidyasagar, A.; Lutkenhaus, J. Fabrication and Thermal Analysis of Layer-by-Layer Micro- and Nanotubes. *Curr. Opin. Colloid Interface Sci.* **2012**, *17*, 114–121.
26. Wang, Y.; Angelatos, A.; Caruso, F. Template Synthesis of Nanostructured Materials *via* Layer-by-Layer Assembly. *Chem. Mater.* **2008**, *20*, 848–858.
27. Jang, W. S.; Saito, T.; Hickner, M. A.; Lutkenhaus, J. L. Electrostatic Assembly of Poly(ethylene glycol) Nanotubes. *Macromol. Rapid Commun.* **2010**, *31*, 745–751.
28. Boulmedais, F.; Frisch, B.; Etienne, O.; Lavalle, P.; Picart, C.; Ogier, J.; Voegel, J. C.; Schaaf, P.; Egles, C. Polyelectrolyte Multilayer Films with Pegylated Polypeptides as a New Type of Anti-Microbial Protection for Biomaterials. *Biomaterials* **2004**, *25*, 2003–2011.
29. Grunlan, J. C.; Choi, J. K.; Lin, A. Antimicrobial Behavior of Polyelectrolyte Multilayer Films Containing Cetrimide and Silver. *Biomacromolecules* **2005**, *6*, 1149–1153.
30. Lee, D.; Cohen, R. E.; Rubner, M. F. Antibacterial Properties of Ag Nanoparticle Loaded Multilayers and Formation of Magnetically Directed Antibacterial Microparticles. *Langmuir* **2005**, *21*, 9651–9659.
31. Wood, K. C.; Boedicker, J. Q.; Lynn, D. M.; Hammond, P. T. Tunable Drug Release from Hydrolytically Degradable Layer-by-Layer Thin Films. *Langmuir* **2005**, *21*, 1603–1609.
32. Laufer, G.; Kirkland, C.; Cain, A. A.; Grunlan, J. C. Clay-Chitosan Nanobrick Walls: Completely Renewable Gas Barrier and Flame-Retardant Nanocoatings. *ACS Appl. Mater. Interfaces* **2012**, *4*, 1643–1649.
33. Priolo, M. A.; Gamboa, D.; Holder, K. M.; Grunlan, J. C. Super Gas Barrier of Transparent Polymer-Clay Multilayer Ultrathin Films. *Nano Lett.* **2010**, *10*, 4970–4974.
34. Kim, D.; Tzeng, P.; Barnett, K. J.; Yang, Y. H.; Wilhite, B. A.; Grunlan, J. C. Highly Size-Selective Ionically Crosslinked Multilayer Polymer Films for Light Gas Separation. *Adv. Mater.* **2014**, *26*, 746–751.
35. Bruening, M. L.; Dotzauer, D. M.; Jain, P.; Ouyang, L.; Baker, G. L. Creation of Functional Membranes Using Polyelectrolyte Multilayers and Polymer Brushes. *Langmuir* **2008**, *24*, 7663–7673.
36. Stanton, B.; Harris, J.; Miller, M.; Bruening, M. Ultrathin, Multilayered Polyelectrolyte Films as Nanofiltration Membranes. *Langmuir* **2003**, *19*, 7038–7042.

37. Yaroshchuk, A.; Bruening, M. L.; Bernal, E. E. L. Solution-Diffusion-Electro-Migration Model and Its Uses for Analysis of Nanofiltration, Pressure-Retarded Osmosis and Forward Osmosis in Multi-Ionic Solutions. *J. Membr. Sci.* **2013**, *447*, 463–476.
38. Armstrong, J. A.; Bernal, E. E. L.; Yaroshchuk, A.; Bruening, M. L. Separation of Ions Using Polyelectrolyte-Modified Nanoporous Track-Etched Membranes. *Langmuir* **2013**, *29*, 10287–10296.
39. Balachandra, A.; Dai, J.; Bruening, M. Enhancing the Anion-Transport Selectivity of Multilayer Polyelectrolyte Membranes by Templating with Cu^{2+}. *Macromolecules* **2002**, *35*, 3171–3178.
40. Sheng, C. J.; Wijeratne, S.; Cheng, C.; Baker, G. L.; Bruening, M. L. Facilitated Ion Transport through Polyelectrolyte Multilayer Films Containing Metal-Binding Ligands. *J. Membr. Sci.* **2014**, *459*, 169–176.
41. Liang, Z.; Susha, A. S.; Yu, A.; Caruso, F. Nanotubes Prepared by Layer-by-Layer Coating of Porous Membrane Templates. *Adv. Mater.* **2003**, *15*, 1849–1853.
42. Ai, S.; Lu, G.; He, Q.; Li, J. Highly Flexible Polyelectrolyte Nanotubes. *J. Am. Chem. Soc.* **2003**, *125*, 11140–11141.
43. Cho, Y.; Lee, W.; Jhon, Y.; Genzer, J.; Char, K. Polymer Nanotubules Obtained by Layer-by-Layer Deposition within AAO-Membrane Templates with Sub-100-nm Pore Diameters. *Small* **2010**, *6*, 2683–2689.
44. Xue, J.; Xie, Y.; Yan, Y.; Ke, J.; Wang, Y. Surface Charge Density of the Track-Etched Nanopores in Polyethylene Terephthalate Foils. *Biomicrofluidics* **2009**, *3*, 022408.
45. Xie, H.; Saito, T.; Hickner, M. Zeta Potential of Ion-Conductive Membranes by Streaming Current Measurements. *Langmuir* **2011**, *27*, 4721–4727.
46. Sham, A.; Notley, S. Layer-by-Layer Assembly of Thin Films Containing Exfoliated Pristine Graphene Nanosheets and Polyethyleneimine. *Langmuir* **2014**, *30*, 2410–2418.
47. Elzbieciak, M.; Zapotoczny, S.; Nowak, P.; Krastev, R.; Nowakowska, M.; Warszynski, P. Influence of pH on the Structure of Multilayer Films Composed of Strong and Weak Polyelectrolytes. *Langmuir* **2009**, *25*, 3255–3259.
48. Baker, R. W. *Membrane Technology and Applications*, 2nd ed.; J. Wiley: Chichester, 2004.
49. Ouyang, L.; Malaisamy, R.; Bruening, M. L. Multilayer Polyelectrolyte Films as Nanofiltration Membranes for Separating Monovalent and Divalent Cations. *J. Membr. Sci.* **2008**, *310*, 76–84.
50. Phillip, W. A.; Amendt, M.; O'Neill, B.; Chen, L.; Hillmyer, M. A.; Cussler, E. L. Diffusion and Flow across Nanoporous Polydicyclopentadiene-Based Membranes. *ACS Appl. Mater. Interfaces* **2009**, *1*, 472–480.
51. Yossifon, G.; Mushenheim, P.; Chang, Y. C.; Chang, H. C. Eliminating the Limiting-Current Phenomenon by Geometric Field Focusing into Nanopores and Nanoslots. *Phys. Rev. E* **2010**, *81*, 046301.
52. Lazzara, T.; Lau, K.; Abou-Kandil, A.; Caminade, A.; Majoral, J.; Knoll, W. Polyelectrolyte Layer-by-Layer Deposition in Cylindrical Nanopores. *ACS Nano* **2010**, *4*, 3909–3920.